Scientia Africana, Vol. 19 (No. 3), December, 2020. Pp 167-180 https://dx.doi.org/10.4314/sa.v19i3.12
© Faculty of Science, University of Port Harcourt, Printed in Nigeria *ISSN 1118 – 1931*

STRUCTURAL, ELECTRONIC, MECHANICAL AND THERMODYNAMIC PROPERTIES OF HALF-METALLIC RH_2FEZ (Z = GA, IN) FULL HEUSLER COMPOUNDS FROM FIRST PRINCIPLES

O. E. Osafile* and J. O. Umukoro

Department of Physics, Federal University of Petroleum Resources, PMB 1221, Effurun, Nigeria
*Corresponding author E-mail address: osafile.omosede@fupre.edu.ng

Received: 09-10-2020
Accepted: 22-10-2020

ABSTRACT

We report on the structural, electronic, mechanical, and thermodynamic properties of Rh_2FeGa and Rh_2FeIn full Heusler alloys from first principles. Results for the structural analysis establishes structural stability with a negative formation energy of -0.2175 eV and -0.2082 eV for Rh_2FeGa and Rh_2FeIn, respectively. The lattice constants and electronic properties compare favorably with reports from existing literature. The compounds are both anisotropic and mechanically stable, having checked out with the Born and Huang criteria. Rh_2FeIn alloy is more ductile, yet, harder, and stiffer compared to its Rh_2FeGa counterpart. The Debye temperatures of 400.124 K and 267. 738 K recorded for Rh_2FeGa and Rh_2FeIn, respectively, is consistent with the expectation that the main group element's atomic size has an inverse relationship with the Debye temperature. Therefore, indium with the larger atomic size has a lesser Debye temperature. Both compounds obey the Dulong-Petit limit at temperatures between 400 K and 500 K. The specific heat capacity at constant volume C_v of 96.5 $J\,mol^{-1}K^{-1}$ *and* 98 $J\,mol^{-1}K^{-1}$ *for Rh_2FeIn and Rh_2FeGa alloys suggests thermodynamic stability of the compounds at moderate temperatures.*

Keywords: Density functional theory; Density functional perturbation theory; Half-Heusler compounds; Mechanical Properties; Thermodynamic properties.

INTRODUCTION

Heusler compounds are a family of ternary inter-metallics with a 2:1:1 stoichiometry for the full Heusler compounds and they generally crystallize in the cubic structure (Fm3m, space group no. 225) with Cu_2MnAl ($L2_1$). Several researchers have widely researched this family of alloys because of their highly tunable properties and have put forward some promising results since its discovery in 1903 (Heusler, 1903). They have proven to be promising materials in the area of spintronics (Kandy et al., 2019; Sharma et al., 2019; Palmstrøm, 2016; Hirohata et al., 2020), giant magnetic resonance (Aryal et al., 2020; Ambrose et al., 2000), spin injection devices (Farshchi & Ramsteiner, 2013; seki et al., 2014; Bruskt et al., 2013), electromechanical applications (Enkovaara et al., 2004), tunneling magnetoresistance in magnetic tunneling junctions and for highly-sensitive Hall sensors due to the unusual inherent Hall conductance among others (Galanakis & Dederichs, 2005).

The Wyckoff positions of the atoms Z, Y in a fully ordered primitive cell of the $L2_1$ structure occupies positions 4a (0, 0, 0), 4b (1/2, 1/2, 1/2), and X occupy positions 4c (1/4, 1/4, 1/4) and 4d (3/4, 3/4, 3/4)

respectively. There is, however, the possibility of a disorder. In the full Heusler compound, atoms occupy all lattice sites, unlike the half Heusler alloy where one site (either the 4d or the 4d sites) is vacant. This family of alloys has the chemical formula X_2YZ. They exhibit dynamic physical, electronic, structural, thermodynamic, mechanical, and magnetic properties and can be semiconductors, metals, topological insulators, half-metals, or semi-metals. The properties exhibited by the full Heusler alloys depend on the elements, the composition of the elements, and a plethora of other thermo- and electro-physical properties of the compound.

They are predominantly ferromagnetic, with some exceptions. Research has proven that the number of valence electrons contributes immensely to the magnetic characterization of the alloys (Edström et al., 2015; Patel et al., 2019; Osafile et al., 2017). On this strength, Slater-Pauling, in their work, showed that the valency of the alloy could accurately predict the magnetic moment of a Heusler compound and, in turn, lend credence to the possibilities of half-metallicity in the compounds, this is known as the Slater-Pauling rule (SP-rule) (Galanakis et al., 2002; Luo et al., 2011). According to the SP-rule, alloys with integer magnetic moments per unit cell are predicted to be half-metallic and mostly exhibit 100% spin polarization (this does not always hold). The SP-rule for the full Heusler alloy is given as $M_t = Z_t - 24$. SP-rule is a rather important characteristic in the stoichiometric composition of the compounds because a small deviation from unity or an integer value of the magnetic moment per unit cell could result in a significant disruption in the half-metallic character by a non-zero electronic density of states for minority spins around the Fermi level (Kandpal et al., 2006; Candan et al., 2013).

The highly tuneable properties of the Heusler family of alloys have made it quite attractive and have led to the discovery of several possible technological applications of the full Heusler compounds. Basic knowledge of the structural, electronic, optical, magnetic, vibrational, thermal, elastic, and mechanical properties of a compound is required in deference to the compound's desired application. In response to this, there are several literature reports from experiments and first-principles on fundamental properties like structural, electronic, and magnetism. From ab-initio, these properties aid in predicting the stability of the compounds and possible applications (Galanakis & Mavropoulos, 2007; Palmstrøm, 2003; Rached et al., 2009; Jiang et al., 2019; Maafa et al., 2020). Other dynamic properties like lattice dynamics, mechanical properties, thermodynamic properties, optical properties, and thermoelectric properties for recently predicted full Heusler compounds are limited in literature (Ram et al., 2020; Hao et al., 2019; Inomata et al., 2006; Kurtulus et al., 2005; Gilleßen & Dronskowski, 2009; Okamura et al., 2004). For Rh based alloys, Galanakis et al. in their investigations using the Vosko, Wilk and Nusair parameterization for the local density approximation (LDA) to the exchange-correlation potential to solve the Kohn-Sham equations within the full-potential screened Korringa-Kohn-Rostoker (FSKKR) method reported on Rh_2MnZ (Z = Al, Ga, In, Tl, Ge, Sn, Pb) Rh based full Heusler alloy. They predicted half-metallic behaviour in Rh_2MnAl and Rh_2MnGa compounds (Galanakis et al,

Scientia Africana, Vol. 19 (No. 3), December, 2020. Pp 167-180 https://dx.doi.org/10.4314/sa.v19i3.12
© Faculty of Science, University of Port Harcourt, Printed in Nigeria *ISSN 1118 – 1931*

2002). The LDA method underestimates the bandgap of most Heusler alloys. It is however, expected that the interaction of Fe and Mn with Rh will be comparable considering the electronic configuration of both elements. The half-metallic property was also reported for Rh_2ZrX (X = Si, Ge, Sn) among the six compounds studied by Ahmad et al. using PBE-GGA and PBE-GGA+U in the quantum espresso suite (Abadi et al., 2019). Boumia et al. investigated the structural, electronic and magnetic properties of Rh_2CrZ (Z = Al, Ga, In) Heusler alloys from first principles based on the density functional theory (DFT) within the full-potential linearized augmented plane wave method (FP-LAPW). They predicted the Rh based alloys to be half-metallic compounds positioning it for application in spintronics. They equally buttressed the compound's stability by computing the formation energy using Tran and Blaha modified Becke-Johnson (TB-mBJ) potential and GGA + U (Boumia et al., 2019). Using the Wien2k code, Monir et al. reported on the novel Rh_2FeGa and Rh_2FeIn full Heusler alloys using the ab initio method of full-potential linearized plane waves plus local orbital based on the framework of density functional theory, within the spin generalized gradient approximation plus U (GGA+U), where U is the Hubbard on-site correction term for exchange-correlation potential. They predicted the alloys to be ferromagnetic with indirect bandgap from $\Gamma \rightarrow X$ in the minority spin band. Furthermore, they submitted that both compounds are half-metallic compounds (Monir et al., 2018).

There is no report, however, on the formation energy, elastic properties, lattice dynamics, and mechanical properties of Rh_2FeZ (Z = Ga, In) alloys to the best of our knowledge. The knowledge of these properties is necessary to fully exploit these alloys' technological applications and ascertain their stability. Against this background, we investigate the structural, electronic, elastic, mechanical, and thermodynamic properties of Rh_2FeGa (In) to establish the alloys' stability and posit possible applications in this paper. Results obtained for the structural and electronic properties are compared with results in the work of Monir et al. (2018).

In section 2, we report the computational technique used for all calculations. Section 3 focuses on reporting and discussing the results for the electronic properties (band structure and density of states), elastic properties, mechanical properties, and thermodynamic properties. We finally submit our conclusions in section 4.

COMPUTATIONAL METHOD

We implemented two levels of computational theory in this work. These are the density functional theory (DFT) calculation and the linear response density functional perturbation theory (DFPT) calculation (Hohenberg & Kohn, 1964; Baroni et al. 1987). The lattice parameter, cut-off energy, electronic charge density, and the K-point were first structurally optimized to obtain the equilibrium values. We performed the structural calculations via the plane augmented wave based on the DFT as implemented in the quantum ESPRESSO suite (Giannozzi et al., 2009). We computed the structural, electronic, and magnetic properties of the alloys using the generalized gradient approximation of Perdew-Burke-Ernzerhof (PBE-GGA) (Perdew et al., 1996; Perdew et al., 1996; Madsen, 2007). On the strength of the existing results by Monir et al, we treated

both structures as ferromagnetic face-centered cubic structures. By structural optimization, we obtained and used the converged values of 70 Ry and 700 Ry as the energy cut-off for expanding the eigenfunctions and the electronic charge density, respectively. Symmetry operations were engaged to reduce the equilibrium 11 x 11 x 11 mesh with 56 k-points for the self-consistent functional (SCF) and the denser grid of 22 x 22 x 22 with 100 k-points for the density of states calculation. We used the smearing technique with a parameter of 0.02 Ry for the Fermi surface integration while the tetrahedra method was used for the density of states calculation.

Furthermore, we investigated the elastic properties, phonon dispersions, density of states, and mechanical properties of the alloys using the linear response density-functional perturbation theory. We performed the phonon calculations using a 2 x 2 x 2 q-point mesh in the quasi-harmonic approximation. A Fourier deconvolution was performed on the mesh to evaluate the dynamical matrices at the gamma point.

RESULTS AND DISCUSSION

Structural and Electronic Properties

We investigated Rh_2FeGa and Rh_2FeIn full Heusler alloys in $L2_1$ (Cu_2MnAl- type) structure and XA (Hg_2CuTi-type) structure. Figure 1 shows the convergence of the lattice parameter for Cu_2MnAl-type and Hg_2CuTi-type for Rh_2FeGa and Rh_2FeIn for $L2_1$ crystal structure. The Figure shows that both compounds crystallize in the Cu_2MnAl-type $L2_1$ face-centered cubic crystal structure with space group number 225 and the Fm3m structure as ferromagnets as expected in cases where the valency of the X atom is greater than the valency of the Y atom in full Heusler compounds. In the Cu_2MnAl structure, X atoms occupy 4a $(0,0,0)$ and 4b $(\frac{1}{2},\frac{1}{2},\frac{1}{2})$ sites while Y and Z atoms occupy 4c $\left(\frac{1}{4},\frac{1}{4},\frac{1}{4}\right)$and 4d $\left(\frac{3}{4},\frac{3}{4},\frac{3}{4}\right)$ sites respectively. The electronic configurations of the compounds (valency) of the compounds read as Rh ($5s^1 4d^8$), Fe ($4s^2 3d^6$), Ga ($4s^2 4p^1$), and In ($5s^2 5p^1$). The electronic configuration implies that Rh_2FeGa and Rh_2FeIn alloys both have a valency of 29 and, hence will have a total magnetic moment per formula unit of 5 μB.

We ascertained the equilibrium structure of the compounds using the convergence of the lattice constant by fitting the computed results for a range of lattice parameters (-0.6 – Z – +0.6) in steps of 0.1 (where Z is a carefully assumed lattice parameter number), to the third Murnaghan equation of state (Hao et al., 2019) represented by Equation (1) in terms of energy and volume.

$$\Delta E(V) = E - E_0 = BV_0\left[\left(\frac{V_n}{B'}\right) + \left(\frac{1}{1-B'}\right) + \left(\frac{V_n}{B'(B'-1)}\right)\right] \quad (1)$$

$E_0$and V_0 are equilibrium values of energy and volume, respectively, without the effect of pressure. Band B' denotes the bulk modulus and its derivative, respectively.

Scientia Africana, Vol. 19 (No. 3), December, 2020. Pp 167-180 https://dx.doi.org/10.4314/sa.v19i3.12
© Faculty of Science, University of Port Harcourt, Printed in Nigeria *ISSN 1118 – 1931*

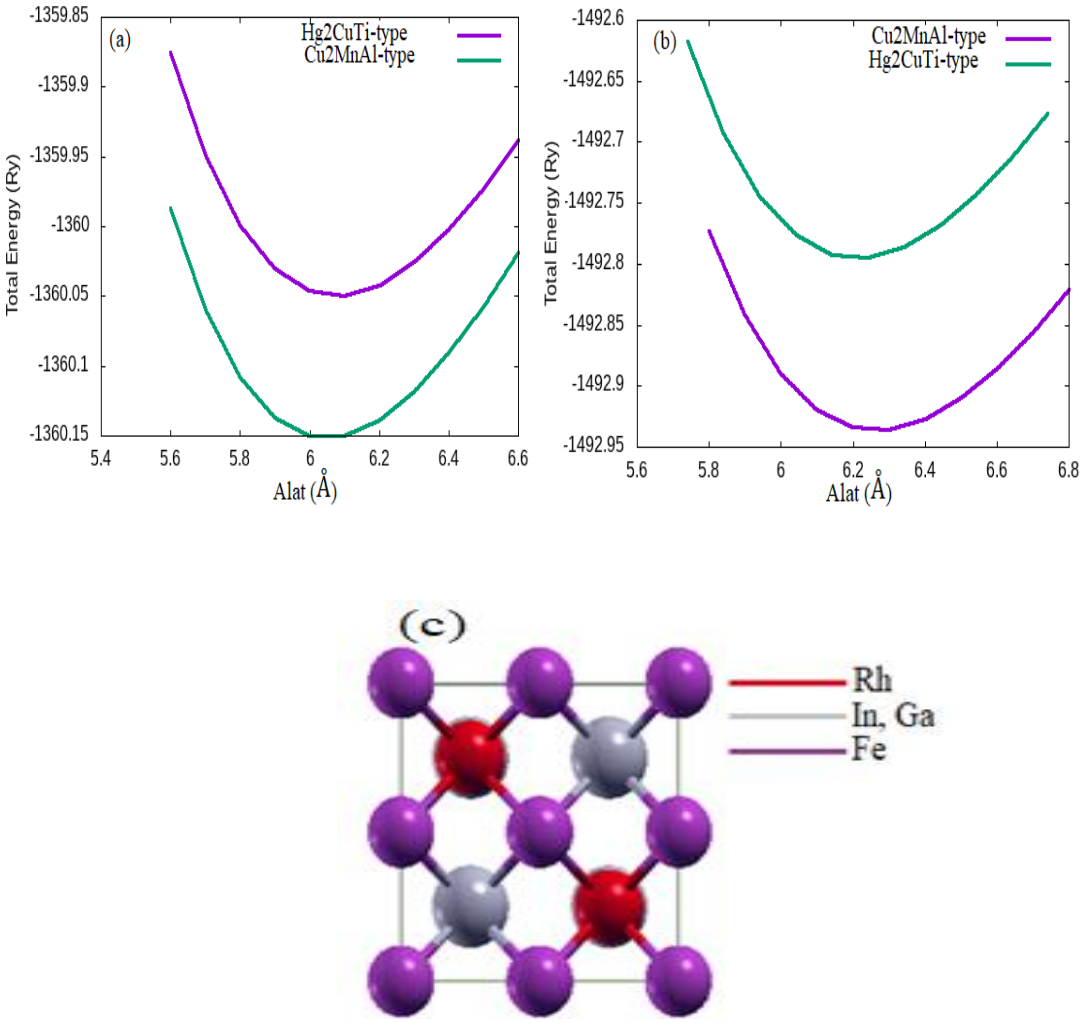

Fig. 1. Lattice parameter optimization curve for (a) Cu_2MnAl-type and Hg_2CuTi-type in Rh_2FeGa alloy (b) Cu_2MnAl-type and Hg_2CuTi-type in Rh_2FeIn alloy (c) $L2_1$ crystal structures of the conventional Rh_2FeZ (Z = Ga, In) alloys viewed via XcrySDen

In Table 1, we present the equilibrium lattice constant, bulk modulus, derivative of the bulk modulus, formation energy, and the bandgap at ambient temperature and zero pressure using PBE-GGA approximation. The results for the lattice constant are in reasonable agreement with results reported in the work of Monir et al. We obtained the formation energy using Equation (2)

$$E_{form} = \frac{1}{4}[E_0 - (2E_{Rh} + E_{Fe} + E_Z)] \quad (2)$$

E_0 denotes the ground-state energy of Rh_2FeZ (Z = Ga, In) alloy, E_{Rh}, and E_{Fe} are the equilibrium energies of rhodium and iron, respectively, while, E_Z is the equilibrium energy of either Gallium or indium in their default structures. From the negative formation energies of -0.2172 and -0.2088 for Rh_2FeGa and Rh_2FeInrespectively in Table 1, we can infer that both compounds are structurally stable and can be synthesized experimentally.

Rh_2FeGa and Rh_2FeIn compound both exhibit half-metallic properties with a narrow bandgap in the minority spin band and metallic behaviour in the majority spin band, as is seen in Figs. 2

& 3 for the electronic density of states (DOS) and the band structure of the compounds. The half-metallic property corroborates the result reported in the work of Monir et al. of the half-metallic behaviour of the alloys.

Table 1 Results obtained from PBE-GGA for the equilibrium lattice constant a_0 (Å), bulk modulus $B_0(GPa)$, pressure derivative of the bulk modulus B_0', formation energy E_{form} *(Ry)*, and bandgap E_g *(eV)* of Rh_2FeGa and Rh_2FeIn full Heusler alloys and compared with existing results (Monir et al., 2018) in the 2nd and 4th row of Table 1.

compound	a_0 (Å)	B_0(GPa),	B_0'	E_{form} (Ry)	E_g (eV)
Rh_2FeGa	6.0471	193.3	4.91	-0.2175	0.282
	6.0411	203.3123	4.9238		
Rh_2FeIn	6.2682	168.3	4.63	-0.2082	0.195
	6.2447	191.4996	4.4358		

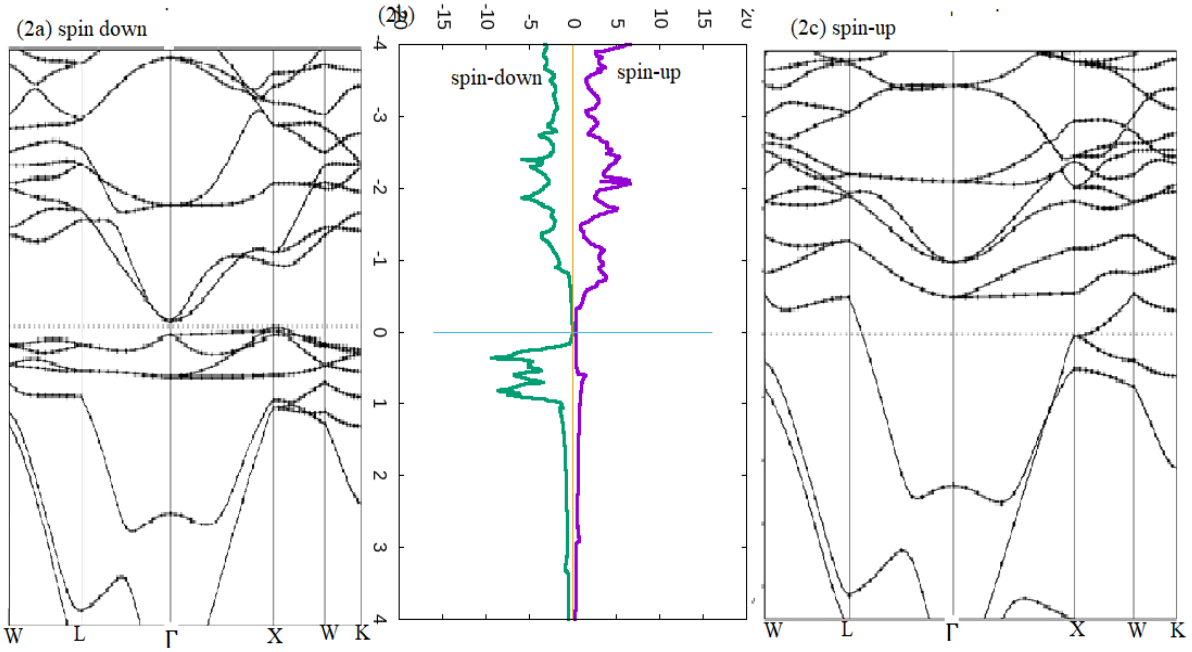

Fig. 2. (2a) Band structure for the minority band (2b) spin-polarized density of states for the majority and minority band (2c) band structure for the majority band of Rh2FeGa alloy using PBE-GGA

Scientia Africana, Vol. 19 (No. 3), December, 2020. Pp 167-180 https://dx.doi.org/10.4314/sa.v19i3.12
© Faculty of Science, University of Port Harcourt, Printed in Nigeria *ISSN 1118 – 1931*

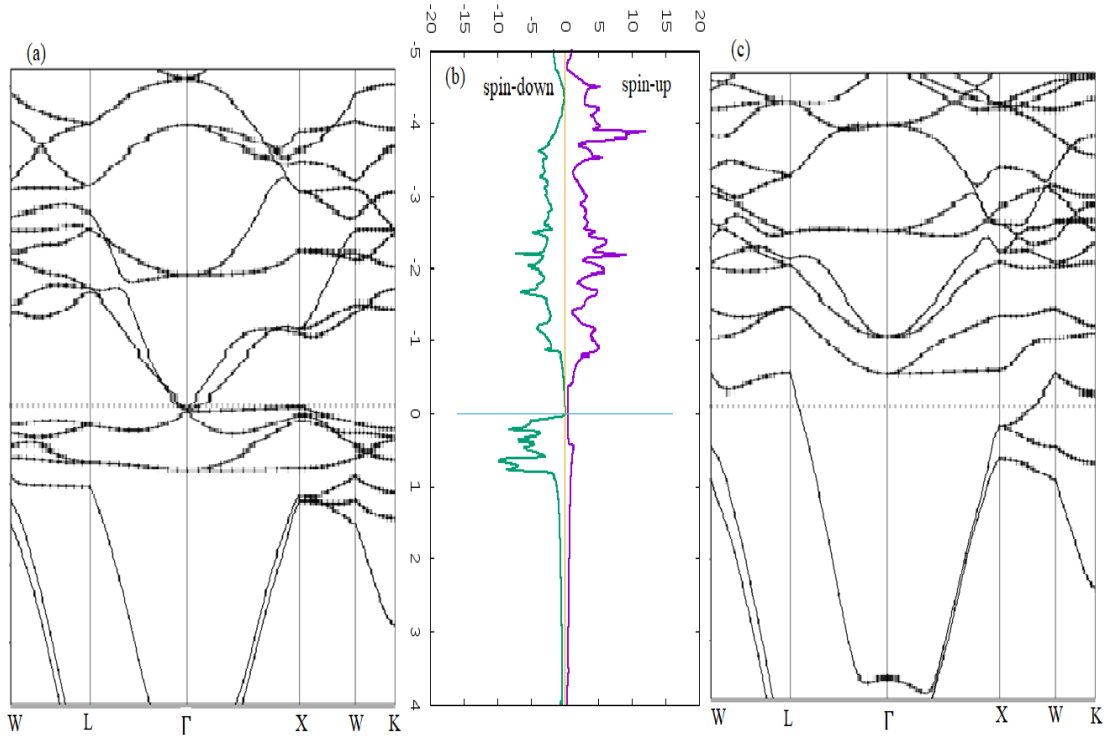

Fig. 3. (a) Band structure for the minority band (3b) spin-polarized density of states for the majority and minority band (3c) band structure for the majority band of Rh_2FeIn alloy using PBE-GGA

Elastic and Mechanical Properties

We analysed the elastic properties of the materials in a bid to establish the mechanical stability of the compounds investigated. the Born stability criteria (Born & Huang, 1954) is the generally accepted condition for mechanical stability for cubic structures, and it is given in Eqn. (3) as

$$\left.\begin{array}{l} C_{11} > 0; C_{44} > 0 \\ \frac{1}{2}(C_{11} - C_{12}) > 0 \\ \frac{1}{3}(C_{11} + 2C_{12}) > 0 \end{array}\right\} \quad (3)$$

the parameters $C_{11} + 2C_{12}$, $C_{11} - C_{12}$, and C_{44} represents the non-degenerate, two-fold degenerate and three-fold degenerate levels of the bands in a cubic system. The three parameters correspond to the bulk, tetragonal shear, and the shear moduli of the crystal, and the cubic crystals become unstable if these values become negative (Inomata et al., 2006). It is, furthermore, required that $C_{12} < B < C_{11}$. Other elastic properties considered are bulk, shear, and young moduli. Computation of the moduli properties was performed using the following Equations.

$$B = \frac{1}{3}(C_{11} + 2C_{12}) \quad (4)$$

$$G = \frac{1}{2}(G_V + 2G_R) \quad (5)$$

$$E = \frac{9BG}{3B+G} \quad (6)$$

the G_V and G_R in Eqn. (6) are the Voigt and Reuss approximations of the shear modulus, respectively, and are obtained using.

$$G_V = \frac{1}{5}(C_{11} - C_{12} + 3C_{44}) \quad (7)$$

$$G_R = 5\frac{(C_{11}-C_{12})C_{44}}{3(C_{11}-C_{12})+4C_{44}} \quad (8)$$

the bulk modulus *B* characterizes the ability of a material to resist fracture and, hence, defines the hardness of the material, the shear modulus G defines the resistance of the material to plastic deformations. The Young's modulus E, on the other hand, is the ratio of tensile stress to tensile strain, and it measures the stiffness of the material. We calculated the moduli using the Voigt and Reuss approximation. These are all derived directly from C_{11}, C_{12}, and C_{44}, the relevant elastic parameters for a cubic crystal structure. C_{11} and C_{44} describe the degree of material's stiffness against principal strains and the stiffness of a crystal structure, which determines the resistance against shear deformation, respectively.

From the results presented in Table. 2, Rh_2FeGa alloy will resist fracture more than Rh_2FeIn; it is a harder and a stiffer material and will resist plastic deformation more than its Rh_2FeIn counterpart. We also compute and present results in Table 2. for anisotropy, Poisson ratio, the Pugh's ratio (B/G) for ductility/brittleness, Cauchy's pressure, and Vick's hardness using Eqns. (9-12);

$$A = \frac{2C_{44}}{C_{11}-C_{12}} \quad (9)$$

$$\upsilon = \frac{1}{2}\left(\frac{3B-2G}{3B+G}\right) \quad (10)$$

$$C^P = C_{12} - C_{44} \quad (11)$$

$$H_V = 0.92\left({}^{B}/_{G}\right)^{1.3137} G^{0.708} \quad (12)$$

where A, υ, C^P, and H_V are the anisotropy factor, Poisson ratio, Cauchy pressure, and the Vicker's hardness. The Poisson ratio and the Cauchy pressure suggests the possible bonding of the atoms in the compound. Frantsevich et al. (1982), in their work, reported a critical value of 0.26 for the Poisson ratio. This critical value separates between a covalent bonding and an ionic bonding, from the results in Table 2, the values favours ionic bonding in both compounds. A sizeable negative C^P supports directional covalent bonding, while a positive value suggests non-directional metallic bonding. Results for the compounds are both positive and substantial, hence, supporting a non-directional metallic bonding among the atoms. In isotropic materials, the properties of the material are independent of the direction, while the material properties are direction-dependent in anisotropic materials. When a material is measured from different directions, any deviation from unity automatically renders the material anisotropic. The values of the anisotropy/isotropy test for the materials are 1.9286 (5.8219) for Rh_2FeGa (In) respectively, the result shows, they are both anisotropic. However, Rh_2FeGa will endure cracking when undergoing experimental growth compared to Rh_2FeIn alloy, because the more extensive the deviation from unity, the more susceptible it is to cracks during experimental growth.

Pugh (2009) established 1.75 at the critical value from the ratio of bulk modulus to the shear modulus (B/G) of a material to be the reference value between brittleness and ductility in a material. When the B/G value is below/above the reference value, the material is brittle/ductile. The brittleness or

Scientia Africana, Vol. 19 (No. 3), December, 2020. Pp 167-180 https://dx.doi.org/10.4314/sa.v19i3.12
© Faculty of Science, University of Port Harcourt, Printed in Nigeria *ISSN 1118 – 1931*

ductility of a material can affect the failure mode in fabrication processes. The results in Table 2 show that both materials are ductile, with Rh_2FeIn more ductile than Rh_2FeGa despite the hardness. The Vicker's hardness holistically addresses resistance of the material to indentation. It addresses this concerning the chemical bonding within the entire compound. Tian et al. predict that materials whose Vicker's hardness is above 40 GPa are super-hard materials. Against this background, our results show that both materials are super-hard with Rh_2FeIn alloy harder than Rh_2FeGa alloy.

Table 2 Calculated elastic constant parameters (C_{11}, C_{12}, C_{44}), the stability conditions ($C_{11} - C_{12}, C_{11} + 2C_{12}$) bulk modulus (B), shear modulus (G), Young modulus (E), elastic anisotropy (A), Poisson's ratio (ν), Cauchy's pressure (C^P), Pugh's ratio (B/G), and Vickers hardness (H_V)

Parameters (GPa)	Rh_2FeGa	Rh_2FeIn
C_{11}	284.5502	192.0201
C_{12}	171.4955	162.4319
C_{44}	109.0182	86.1303
$C_{11} - C_{12}$	113.5461	29.5882
$C_{11} + 2C_{12}$	627.5413	51.6883
B	209.1804	172.2946
G	83.7569	43.5020
E	221.6233	119.4698
A	1.9286	5.8219
ν	0.3230	0.3732
B/G	2.4975	3.9606
C^P	62.4773	76.3016
H_V	70.3839	81.1208

Thermodynamic properties

Resulting from our interest in the behavior of RhFeGa(In) alloys in the low- and high-temperature limit, we employed the quasi-harmonic approximation (QHA) as against the harmonic approximation because the harmonic approximation cannot account for thermal expansion and thermal transport as the temperature increases, and does not respond to phonon interaction; hence the phonon lifetime is interpreted as infinite. To implement the QHA, the *X-factor* is introduced into the harmonic approximation of the vibrational Helmholtz energy, where X represents the lattice parameter or the volume. Hence, we have the relation for the QHA from the vibrational Helmholtz energy (F^{vib}) as:

$$F^{vib}(X,T) = \frac{1}{2N}\sum_{\vec{q},\upsilon}\hbar\omega\,(\vec{q},\upsilon,X) + \frac{k_BT}{N}\sum_{\vec{q},\upsilon} In\left[1 - exp\left(\frac{-\hbar\omega(\vec{q},\upsilon,X)}{k_BT}\right)\right] \quad (13)$$

where q is the wave-vector, the vibrational frequency is ω(q), k_B is the Boltzmann constant, T is temperature, $\hbar$ is the reduced Planck's constant, and υ is the frequency.

One drawback of QHA is its inability to account for anharmonicity in its entirety at high temperatures (Tian et al., 2012; Anderson, 1963). There is, however, enough information between temperatures of 0 K and 800 K studied in this work to make reasonable predictions about the materials investigated. The parameters are all reported at zero pressure, and these include the Debye temperature Θ_D, specific heat capacity at constant volume C_v and its relation to the Dulong-Petit law, the average mean velocity, and the Debye entropy. The Debye temperature throws light on the thermal properties of the material at high temperature or pressure. In Table 3, we present the sound velocities (shear, compressional, and bulk) with respect to the temperature, the average sound velocity, and the Debye temperature. We computed the Debye temperature from the average mean velocity of sound using:

$$\Theta_D = \frac{h}{K_B}\left[\frac{3n}{4\pi}\frac{N_A\rho}{M}\right]^{1/3} \nu_m \qquad (14)$$

where h is Planck's constant, K_B is Boltzmann's constant, n is the number of atoms per unit cell, N_A is Avogadro's number, ρ is density, and M is the molecular weight. ν_m is the sound velocity at zero pressure. ν_m can be calculated using the compressional (V_P), and shear (V_G) wave velocities as

$$V_m = \left[\frac{1}{3}\left(\frac{2}{V_G^3} + \frac{1}{V_p^3}\right)\right]^{-1/3} \qquad (15)$$

Navier's Equation [41] provides the relations for obtaining the sound velocities, and we present them in Equations (16 & 17). We present the values obtained from the calculations in Table 3.

$$V_P = \left[\left(B + \frac{4}{3}G\right)\frac{1}{\rho}\right]^{1/2} \qquad (16)$$

$$V_G = \sqrt{\frac{G}{\rho}},\ V_B = \sqrt{\frac{B}{\rho}} \qquad (17)$$

where ρ is the density of the alloy. The wave velocities obtained are as expected when compared to the mass of the alloys investigated. Considering that the mass of Rh_2FeIn is higher than that of Rh_2FeGa, the lighter material with a lighter mass will have a faster sound velocity, as is the case in the result reported in Table 3. The average sound velocity is observed to be higher for Rh_2FeGa alloy. The Debye temperatures of 400.124 K and 267. 738 K is recorded for Rh_2FeGa and Rh_2FeIn, respectively. The result for Θ_D is consistent with the expectation that the atomic size of the main group element has an inverse relationship with ΘD. Therefore, indium with the larger atomic size has a lesser Debye temperature. At 0 GPa and constant volume, the compounds expand rapidly between 0 K and 220 K, as is evident in Fig. 4. The Dulong-Petit limit is achieved at temperatures of about 400 K and 500 K and a C_v of 96.5 $J\ mol^{-1}K^{-1}$ and 98 $J\ mol^{-1}K^{-1}$for Rh_2FeIn and Rh_2FeGa alloys respectively. We present the specific heat capacity at constant volume and the entropy change to temperature in Figs 4a & 4b. As expected, there is a rapid and continuous change in the entropy of the compounds related to temperature, especially between 0 K and 400 K.

Table 3 Results for the Voigt-Reuss-Hill average compressional, bulk and shear sound velocities (V_P, V_B, V_G) in m/s, the average Debye sound velocity υ_m in m/s, and the Debye temperature Θ_D in K of Rh_2FeGa and Rh_2FeIn using QHA

Scientia Africana, Vol. 19 (No. 3), December, 2020. Pp 167-180 https://dx.doi.org/10.4314/sa.v19i3.12
© Faculty of Science, University of Port Harcourt, Printed in Nigeria *ISSN 1118 – 1931*

Parameters	Rh_2FeGa	Rh_2FeIn
V_P (m/s)	5665.336	4759.385
υ_m (m/s)	3220.417	2235.917
V_G (m/s)	2894.547	2068.527
V_B (m/s)	4574.366	4116.633
Θ_D (K)	400.1240	267.738

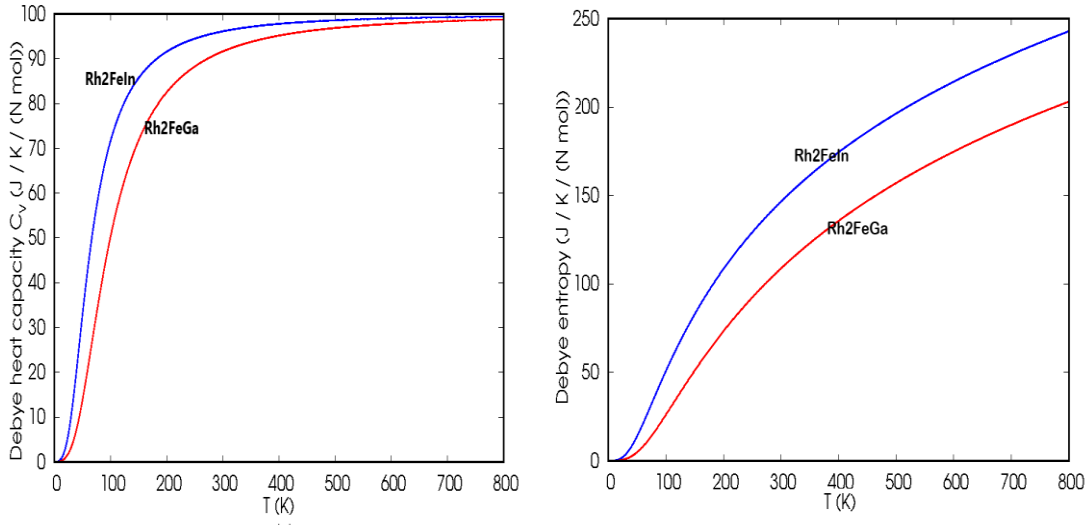

Fig. 4. (a) Debye heat capacity at constant volume of Rh2FeGa and Rh2FeIn alloys using QHA (b) Debye entropy of Rh_2FeGa and Rh_2FeIn alloys using QHA

CONCLUSION

We have investigated the structural and electronic properties of Rh_2FeGa and Rh_2FeIn full Heusler alloys using the density functional theory from the first principles calculation. We have also investigated for the first time, the elastic, mechanical, and thermodynamic properties of the alloys using the density functional perturbation theory. The negative formation energies observed in both alloys establish the possibility of experimental synthesis of the compounds. The results obtained for the lattice parameter compare well with those obtained in the work of Monir et al. (2018). From the electronic structure calculation, both compounds are half-metallic compounds with narrow bandgaps in the minority band and a near integer magnetic moment per unit formula. Rh_2FeGa and Rh_2FeIn compounds both exhibit an indirect bandgap between gamma and X high symmetry points. The results we obtained from the elastic property calculations show that both compounds are mechanically stable, ductile, and hard with Rh_2FeIn more ductile than Rh_2FeGa. Reporting on the hardness, stiffness, and resistance to deformation, Rh_2Fein alloy is harder and stiffer and will be less susceptible to indentation compared to Rh_2FeGa alloy. From the anisotropy of 5.8219 reported for Rh_2FeIn alloy, the compound will be more prone to cracking when subjected to experimental analysis. Both compounds are thermodynamically stable with Debye

temperatures of 400.124 K and 267. 738 K for Rh_2FeGa and Rh_2FeIn, respectively. Both compounds equally obey the Dulong-Petit law at reasonably moderate temperatures. As a further work, the stability of the compounds with respect to temperature should be explored. This is to establish the temperature at which phase transition can occur in the $Rh_2FeGa(In)$ compounds.

REFERENCES

Abadi, A. A. M., Forozani, G., Baizaee, S. M., and Gharaati, A. (2019). Ab Initio Calculations of New Full Heusler Alloys Rh 2 ZrX (X= Al, Ga, In, Si, Ge, Sn). *Journal of Superconductivity and Novel Magnetism*, *32*(8), 2479-2488.

Ambrose, T., Krebs, J. J., and Prinz, G. A. (2000). Magnetic properties of single crystal Co 2 MnGe Heusler alloy films. *Journal of Applied Physics*, *87*(9), 5463-5465.

Anderson, O. L. (1963). A simplified method for calculating the Debye temperature from elastic constants. *Journal of Physics and Chemistry of Solids*, *24*(7), 909-917.

Aryal, A., Bakkar, S., Samassekou, H., Pandey, S., Dubenko, I., Stadler, S., ... and Mazumdar, D. (2020). Mn2FeSi: An antiferromagnetic inverse-Heusler alloy. *Journal of Alloys and Compounds*, *823*, 153770.

Baroni, S., Giannozzi, P., and Testa, A. (1987). Green's-function approach to linear response in solids. *Physical Review Letters*, *58*(18), 1861.

Boumia, L., Dahmane, F., Doumi, B., Rai, D. P., Khandy, S. A., Khachai, H., ... and Khenata, R. (2019). Structural, electronic and magnetic properties of new full Heusler alloys Rh2CrZ (Z= Al, Ga, In): First-principles calculations. *Chinese Journal of Physics*, *59*, 281-290.

Born, M., and Huang, K. (1954). *Dynamical theory of crystal lattices*. Clarendon press.

Bruski, P., Manzke, Y., Farshchi, R., Brandt, O., Herfort, J., and Ramsteiner, M. (2013). All-electrical spin injection and detection in the Co_2FeSi/GaAs hybrid system in the local and non-local configuration. *Applied Physics Letters*, *103*(5), 052406.

Candan, A., Uğur, G., Charifi, Z., Baaziz, H., and Ellialtıoğlu, M. R. (2013). Electronic structure and vibrational properties in cobalt-based full-Heusler compounds: A first principle study of Co_2MnX (X= Si, Ge, Al, Ga). *Journal of alloys and compounds*, *560*, 215-222.

Edström, A., Werwiński, M., Iuşan, D., Rusz, J., Eriksson, O., Skokov, K. P., ... and Fries, M. (2015). Magnetic properties of $(Fe_{1-x}Co_x)_2$ B alloys and the effect of doping by 5d elements. *Physical review B*, *92*(17), 174413.

Enkovaara, J., Ayuela, A., Zayak, A. T., Entel, P., Nordström, L., Dube, M., ... and Nieminen, R. M. (2004). Magnetically driven shape memory alloys. *Materials Science and Engineering: A*, *378*(1-2), 52-60.

Farshchi, R., and Ramsteiner, M. (2013). Spin injection from Heusler alloys into semiconductors: A materials perspective. *Journal of Applied Physics*, *113* (19), 7_1.

Frantsevich, I. N., Voronov, F. F., and Bakuta, S. A. (1982). Elastic constants and elastic moduli of metals and nonmetals (In Russian). *Kiev, Izdatel'stvo Naukova Dumka*, *1982*, *288*.

Galanakis, I., and Dederichs, P. H. (2005). Half-metallicity and Slater-Pauling behavior in the ferromagnetic Heusler alloys. In *Half-metallic Alloys* (pp. 1-39). Springer, Berlin, Heidelberg.

Galanakis, I., Dederichs, P. H., and Papanikolaou, N. (2002). Slater-

Scientia Africana, Vol. 19 (No. 3), December, 2020. Pp 167-180 https://dx.doi.org/10.4314/sa.v19i3.12
© Faculty of Science, University of Port Harcourt, Printed in Nigeria *ISSN 1118 – 1931*

Pauling behavior and origin of the half-metallicity of the full-Heusler alloys. *Physical Review B*, *66*(17), 174429.

Galanakis, I., and Mavropoulos, P. (2007). Spin-polarization and electronic properties of half-metallic Heusler alloys calculated from first principles. *Journal of Physics: Condensed Matter*, *19*(31), 315213.

Giannozzi, P., Baroni, S., Bonini, N., Calandra, M., Car, R., Cavazzoni, C., ... and Dal Corso, A. (2009). QUANTUM ESPRESSO: a modular and open-source software project for quantum simulations of materials. *Journal of physics: Condensed matter*, *21*(39), 395502.

Gilleßen, M., and Dronskowski, R. (2009). A combinatorial study of full Heusler alloys by first-principles computational methods. *Journal of computational chemistry*, *30*(8), 1290-1299.

Hao, L., Khenata, R., Wang, X., and Yang, T. (2019). Ab Initio Study of the Structural, Electronic, Magnetic, Mechanical and Thermodynamic Properties of Full-Heusler Mn_2CoGa. *Journal of Electronic Materials*, *48*(10), 6222-6230.

Heusler, F. (1903). Magnetic manganese alloys. *Verhandl Deuts Phys Ges*, *5*, 219.

Hirohata, A., Yamada, K., Nakatani, Y., Prejbeanu, L., Diény, B., Pirro, P., and Hillebrands, B. (2020). Review on spintronics: Principles and device applications. *Journal of Magnetism and Magnetic Materials*, 166711.

Hohenberg, P., and Kohn, W. (1964). Phys Rev 136: B864. *Kohn W, Sham LJ (1965) Phys Rev*, *140*, A1133.

Inomata, K., Okamura, S., Miyazaki, A., Kikuchi, M., Tezuka, N., Wojcik, M., and Jedryka, E. (2006). Structural and magnetic properties and tunnel magnetoresistance for Co_2(Cr, Fe)Al and Co_2FeSi full-Heusler alloys. *Journal of Physics D: Applied Physics*, *39*(5), 816.

Jiang, D., Ye, Y., Yao, W., Zeng, D., Zhou, J., Liu, L., and Wen, Y. (2019). First-Principles Calculations of the Structural, Magnetic, and Electronic Properties of Fe_2MgB Full-Heusler Alloy. *Journal of Electronic Materials*, *48*(11), 7258-7262.

Kandpal, H. C., Fecher, G. H., Felser, C., and Schönhense, G. (2006). Correlation in the transition-metal-based Heusler compounds Co_2MnSi and Co_2FeSi. *Physical Review B*, *73*(9), 094422.

Khandy, S. A., Islam, I., Gupta, D. C., and Laref, A. (2019). Full Heusler alloys (Co_2TaSi and Co_2TaGe) as potential spintronic materials with tunable band profiles. *Journal of Solid State Chemistry*, *270*, 173-179.

Kurtulus, Y., Dronskowski, R., Samolyuk, G. D., and Antropov, V. P. (2005). Electronic structure and magnetic exchange coupling in ferromagnetic full Heusler alloys. *Physical Review B*, *71*(1), 014425.

Luo, Z., Lim, S., Tian, Z., Shang, J., Lai, L., MacDonald, B., ... and Lin, J. (2011). Pyridinic N doped graphene: synthesis, electronic structure, and electrocatalytic property. *Journal of Materials Chemistry*, *21*(22), 8038-8044.

Maafa, A., Rozale, H., Oughilas, A., Boubaça, A., Amar, A., and Lucache, D. (2020). Theoretical Study of the Electronic Properties of X_2YZ (X= Fe, Co; Y= Zr, Mo; Z= Ge, Sb) Ternary Heusler: Ab-Initio Study. *Annals of West University of Timisoara-Physics*, *1*(ahead-of-print).

Madsen, G. K. (2007). Functional form of the generalized gradient approximation for exchange: The PBE α functional. *Physical Review B*, *75*(19), 195108.

Monir, M. E. A., Ullah, H., Baltach, H., and Mouchaal, Y. (2018). Half-metallic Ferromagnetism in Novel Rh 2-based Full-Heusler Alloys Rh_2FeZ (Z= Ga and In). *Journal of Superconductivity*

and Novel Magnetism, *31*(7), 2233-2239.

Okamura, S., Goto, R., Sugimoto, S., Tezuka, N., and Inomata, K. (2004). Structural, magnetic, and transport properties of full-Heusler alloy $Co_2(Cr_{1-x}Fe_x)Al$ thin films. *Journal of applied physics*, *96*(11), 6561-6564.

Osafile, O. E., Adebambo, P. O., and Adebayo, G. A. (2017). Elastic constants and observed ferromagnetism in inverse Heusler alloy Ti_2CoAs using kjpaw pseudopotentials: A first-principles approach. *Journal of Alloys and Compounds*, *722*, 207-211.

Palmstrøm, C. (2003). Epitaxial Heusler alloys: New materials for semiconductor spintronics. *MRS bulletin*, *28*(10), 725-728.

Palmstrøm, C. J. (2016). Heusler compounds and spintronics. *Progress in Crystal Growth and Characterization of Materials*, *62*(2), 371-397.

Patel, P. D., Shinde, S. M., Gupta, S. D., and Jha, P. K. (2019). A promising thermoelectric response of fully compensated ferrimagnetic spin gapless semiconducting Heusler alloy Zr2MnAl at high temperature: DFT study. *Materials Research Express*, *6*(7), 076307.

Perdew, J. P., Burke, K., and Wang, Y. (1996). Generalized gradient approximation for the exchange-correlation hole of a many-electron system. *Physical Review B*, *54*(23), 16533.

Perdew, J. P., Burke, K., and Ernzerhof, M. (1996). Generalized gradient approximation made simple. *Physical review letters*, *77*(18), 3865.

Pugh, S. F. (1954). XCII. Relations between the elastic moduli and the plastic properties of polycrystalline pure metals. *The London, Edinburgh, and Dublin Philosophical Magazine and Journal of Science*, *45*(367), 823-843.

Rached, H., Rached, D., Khenata, R., Reshak, A. H., and Rabah, M. (2009). First-principles calculations of structural, elastic and electronic properties of Ni2MnZ (Z= Al, Ga and In) Heusler alloys. *physica status solidi (b)*, *246*(7), 1580-1586.

Ram, M., Saxena, A., Aly, A. E., and Shankar, A. (2020). Half-metallicity in new Heusler alloys Mn_2ScZ (Z= Si, Ge, Sn). *RSC Advances*, *10*(13), 7661-7670.

Seki, T., Sakuraba, Y., Arai, H., Ueda, M., Okura, R., Imamura, H., and Takanashi, K. (2014). High power all-metal spin torque oscillator using full Heusler Co2 (Fe, Mn) Si. *Applied Physics Letters*, *105*(9), 092406.

Sharma, M., Das, A., and Kuanr, B. K. (2019). Co-based full Heusler alloy nanowires: Modulation of static and dynamic properties through deposition parameters. *AIP Advances*, *9*(12), 125054.

Tian, Y., Xu, B., Yu, D., Ma, Y., Wang, Y., Jiang, Y., ... and Zhao, Z. (2013). Ultrahard nano-twinned cubic boron nitride. *Nature*, *493*(7432), 385-388